ALPHA-QUENCHED $\alpha^2\Omega$-DYNAMO WAVES IN STELLAR SHELLS

ANDREW SOWARD AND ANDREW BASSOM

School of Mathematical Sciences, University of Exeter, North Park Road, Exeter, Devon EX4 4QE, UK

AND

YANNICK PONTY

Observatoire de la Côte d'Azur, Laboratory Cassini - CNRS UMR 6529, B. P. 4229, 06304 Nice Cedex 4, France

1. Introduction

The generally accepted explanation of the sunspot cycle is in terms of a kinematic $\alpha\Omega$-dynamo wave propagating with fixed period from the pole to the equator (see Parker [1]); for a recent review see Rüdiger and Arlt [2]. Since such oscillatory behaviour is a robust feature generic to all $\alpha\Omega$-dynamo models, the simplicity of the idea is compelling. Both solar and stellar dynamos generally operate in convective spherical shells. There are two limiting cases, namely thick or thin shells as characterised by the ratio ε of the shell thickness to shell radius. In the thick shell limit, it is necessary to consider the full partial differential equations involving the radial and latitudinal dependence. Conversely in the thin shell limit $\varepsilon \ll 1$, it is possible to average the dynamo equations radially leaving a one-dimensional system dependent on the latitude θ alone.

Numerical integrations (Moss *et al.* [3]) of the full partial differential equations governing axisymmetric $\alpha\Omega$-dynamos in the thin shell limit $\varepsilon \ll 1$, upon which we will focus, indicate that there is a short latitudinal length scale comparable to the shell depth. Advantage of this feature was taken by Kuzanyan and Sokoloff [4], who employed WKBJ methods to solve the one-dimensional kinematic $\alpha\Omega$-dynamo system with latitudinally dependent α-effect and differential rotation. This non-uniform background is characterised by local magnetic Reynolds numbers with functional forms $-\varepsilon^{-1}R_\alpha f(\theta)$ and $\varepsilon^{-2}R_\Omega g(\theta)$ respectively; the product of the

dimensionless parameters $-\varepsilon^{-1}R_\alpha$ and $\varepsilon^{-2}R_\Omega$ defines the dynamo number $-\varepsilon^{-3}D := -\varepsilon^{-3}R_\alpha R_\Omega$. The quasi-kinematic extension, in which the α-effect is quenched, was investigated both analytically and numerically by Meunier *et al.* [5]. Strictly the $\alpha\Omega$-dynamo case corresponds to $R_\alpha \to 0$. When R_α is finite, the dynamo is of $\alpha^2\Omega$-type, for which Griffiths *et al.* [6] undertook the corresponding analytic development (but see also Meunier *et al.* [7]). In this paper we summarise some of their key results and outline further recent developments, which include new supporting numerical evidence.

Our $\alpha^2\Omega$-dynamo waves are governed by the model equations

$$\left.\begin{array}{l} \dfrac{\partial A}{\partial t} = \alpha B + \varepsilon^2 \dfrac{\partial^2 A}{\partial \theta^2} - A, \\[3mm] \dfrac{\partial B}{\partial t} = \varepsilon D g(\theta) - R_\alpha^2 \left[\varepsilon^2 \dfrac{\partial}{\partial \theta}\left(\alpha \dfrac{\partial A}{\partial \theta}\right) - \alpha A\right] + \varepsilon^2 \dfrac{\partial^2 B}{\partial \theta^2} - B, \end{array}\right\} \quad (1)$$

where, in suitable dimensionless units, t is time, B and $-\varepsilon R_\alpha \partial A/\partial\theta$ are the azimuthal and radial magnetic fields respectively ($|\mathbf{B}|$ is the total field), and the scaled dynamo number

$$D := R_\alpha R_\Omega \qquad (2)$$

has the opposite sign to that often employed. We restrict our discussion to the particular case $f(\theta) := \sin\theta$ and $g(\theta) := 2\cos\theta$ and so introduce the scaled α-effect Reynolds and Dynamo numbers

$$\mathcal{R}(\theta) = R_\alpha \sin\theta \qquad \text{and} \qquad \mathcal{D}(\theta) = D\sin(2\theta), \qquad (3)$$

respectively.

The reduced problem is characterised by the two parameters R_α and D. To understand the nature of the solutions that our numerical integrations of (1) reveal, it is helpful to note the simple steady state solutions with long azimuthal length scales. For them, all θ derivatives in (1) are negligible except in thin boundary layers which have no significant consequences. So restricting attention to the Northern hemisphere, the zero amplitude state bifurcates to $R_\alpha A = B = B_S(\theta)$, where

$$B_S(\theta) := \begin{cases} \pm\sqrt{(\mathcal{R}(\theta) - 1)/2} & \text{on a polar cap} \quad \theta_S < \theta < \pi/2, \\[3mm] 0 & \text{elsewhere on} \quad 0 \le \theta < \theta_S, \end{cases} \qquad (4)$$

and $\theta_S = \sin^{-1}(1/R_\alpha)$. There is a polar boundary layer of latitudinal length scale $O(\varepsilon)$ across which adjustments of A and B are made to meet the polar boundary conditions. There is a boundary layer also at θ_S leading to

exponentially small values of the magnetic field at the equator $\theta = 0$. Consequently the nature of our asymptotics means that we cannot comment on symmetry as we are unable to distinguish between dipole and quadrupole parity. This is a general feature of the thin shell limit which is not restricted to these particular α^2-dynamo modes. Only for thick shells can these important parity issues be addressed (see e.g. Jennings [8] and Tobias [9]).

Our main concern is with the bifurcation to short length scale travelling waves either as a primary bifurcation from the zero amplitude state or as a secondary bifurcation from the steady finite amplitude state (4). For fixed R_α that bifurcation occurs at some critical value $D_c(R_\alpha)$ of the dynamo number D with some critical frequency ω_c. The latitudinal length scale of these modes is $O(\varepsilon)$. We also determine the nature of the fully developed finite amplitude travelling wave states. These are localised at mid-latitudes and can be identified simply by demanding that the magnetic field associated with them decays to zero as both the pole and equator are approached. They also have the generic feature that these (Parker [1]) waves evaporate smoothly at some latitude θ_P at the equatorial end but are terminated abruptly across a front of width $O(\varepsilon)$ (the wave length scale) at some latitude θ_F at the polar end. The presence of fronts in this class of dynamo problems was first identified by Worledge *et al.* [10] in the case of a uniform background state. Much of the underlying analytical theory for our non-uniform background is reviewed by Soward [11].

2. Linear Theory

Since the waves of interest have short $O(\varepsilon)$ length scale, we consider a WKBJ representation of small perturbations locally proportional to

$$\exp(\mathrm{i}\xi)\,, \qquad \text{where} \qquad \xi := \omega t + \varepsilon^{-1}\! \int k \, \mathrm{d}\theta\,. \tag{5}$$

In the case of perturbations to the non-magnetic basic state, the complex frequency ω is related to the complex wave number $k(\theta)$ by the dispersion relation

$$(\mathrm{i}\omega + 1 + k^2)^2 - \mathcal{R}^2(1 + k^2) - \mathrm{i}\mathcal{D}k = 0\,. \tag{6}$$

For perturbations to the steady α^2-dynamo (4), we write

$$[R_\alpha A, B] = B_S(\theta)[1, 1] + [R_\alpha a(\theta), b(\theta)]\exp(\mathrm{i}\xi) \tag{7}$$

and the most important consequence of $B_S \neq 0$ is that the α-effect is quenched. As a result the coefficient of the exponential of the linearised perturbation to

$$R_\alpha \alpha \begin{bmatrix} R_\alpha A \\ B \end{bmatrix} \qquad \text{is} \qquad \frac{1}{\mathcal{R}} \begin{bmatrix} 1 & -(\mathcal{R} - 1) \\ -(\mathcal{R} - 1) & 1 \end{bmatrix} \begin{bmatrix} R_\alpha a \\ b \end{bmatrix}. \tag{8}$$

4

Thus linearising (1) leads, for $\mathcal{R} \geq 1$, to the local dispersion relation

$$[i\omega + 1 + k^2 + (1 - \mathcal{R}^{-1})]^2 - \mathcal{R}^{-1}[1 + k^2 - (1 - \mathcal{R}^{-1})] - i\mathcal{R}^{-2}\mathcal{D}k = 0 \quad (9)$$

which replaces (6) at locations θ, where $B_S(\theta) \neq 0$. Of course, both relations are identical at θ_S, where $\mathcal{R}(\theta_S) = 1$.

In order that the WKBJ solution is a uniformly valid approximation everywhere between the equator and the pole it is necessary that both the complex group velocity and complex phase mixing vanish,

$$\omega_{,k} = 0 , \qquad \omega_{,\theta} = 0 , \qquad \operatorname{Im}\{\omega\} = 0 , \qquad (10)$$

at some θ_c and k_c possibly complex (see Huerre and Monkewitz [12]). These conditions have been applied to the dispersion relation (6). When $R_\alpha = 0$, θ_c is located at $\pi/4$, the local dynamo number maximum, but k_c is complex (see Kuzanyan and Sokoloff [4]). This means that the maximum of the generated magnetic field is localised elsewhere at a lower latitude θ_M (say). As R_α is increased, $\theta_c(R_\alpha)$ moves off the real axis and becomes fully complex like $k_c(R_\alpha)$ (see Griffiths et $al.$ [6]). Otherwise, the characteristics of the solution are similar to the localised $R_\alpha = 0$ $\alpha\Omega$-dynamo wave.

3. Nonlinear Analytic Theory

Weakly nonlinear theory is difficult to implement in the small ε-limit and leads to surprisingly complicated results (see Griffiths et $al.$ [6], Bassom et $al.$ [13]). Its range of applicability is limited to a very small region of parameter space and the results that can be obtained are not that helpful (see Le Dizès et $al.$ [14]).

A more fruitful approach is to study fully developed finite amplitude states. Unlike the marginal small amplitude solutions which are localised in the neighbourhood of some latitude θ_M, the finite amplitude waves exist over the extended range $\theta_P < \theta < \theta_F$. These travelling wave solutions depend locally on the single variable ξ (see (5)) and have amplitude and wavelength $2\pi/k$ (real) which vary with latitude θ. They merge smoothly with the linear WKBJ solutions at θ_P. On the other hand, the simple wave structure just described is lost at θ_F, where the frontal structure depends on both $(\theta - \theta_F)/\varepsilon$ and t explicitly.

In fact the role of the front may be thought of in terms of a wave transition problem. The arrival of the finite amplitude wave at the front leads to linear transmitted and reflected waves. The linear transmitted waves provide the key to the existence of the front itself. According to both (6) and (9), there are four roots for k leading to four distinct WKBJ type solutions. Only those which decay towards the pole are acceptable and the others that grow have to be rejected. This is only achieved when two of the

roots coincide, which is equivalent to the vanishing of the complex group velocity

$$\omega_{,k} = 0 \, . \tag{11}$$

The importance of this frontal condition was identified by Dee and Langer [15] and is now known as the Dee-Langer condition. The double root feature means that the two corresponding WKBJ solutions are disentangled in a thicker transition layer ahead of the front (see Meunier *et al.* [5], Bassom *et al.* [13], Bassom and Soward [16] and also Pier *et al.* [17]).

To determine the finite amplitude solution, the Dee-Langer condition is applied to the linear dispersion relation. For given R_α and D, this leads to explicit values of real ω and θ_F but complex $k(\theta_F)$, when they exist. In one sense the value of the frequency ω is the key to the solution as well as being the focal point of physical applications (see e.g. Rüdiger and Arlt [18]). Once it is determined, the remaining characteristics follow.

For given R_α, the minimum value $D_{\min}$ at which frontal solutions exist is of interest. For $R_\alpha = 0$, it coincides with the critical value; $D_{\min} = D_c$ but for $R_\alpha > 0$, the frontal solutions are subcritical; $D_{\min} < D_c$. From a mathematical point of view this subcriticality is traced to the complex value of θ_c. The fact that θ_c moves further from the real axis signals the stabilising influence of phase mixing on the linear solution; the nonlinear frontal solution relaxes the phase mixing constraint because the Dee-Langer condition is not concerned with $\omega_{,\theta}$.

4. Nonlinear Numerical Results

We integrated the governing equations (1) as an initial problem from an arbitrary seed field. The numerical solutions were computed until the transients had died away leaving a periodic solution. The numerical method used a pseudo–spectral tau–collocation method with the Chebyshev polynomials. The time stepping is performed with a Crank–Nicholson method for the diffusion terms, and the Adams–Bashford method for the remaining terms. All the selected results reported here are for the case

$$\varepsilon = \pi/600 \, , \tag{12}$$

which was employed in the original $R_\alpha = 0$ calculations of Meunier *et al.* [5]. This value is certainly far smaller than is appropriate for solar applications for which ε is about 1/3. We adopt the small value $\pi/600$ to emphasise the asymmetry of the solutions and the frontal structure.

For the case $R_\alpha = 0$, the asymptotics predicts the values $D_c \approx 8.71$, $\omega_c \approx 1.73$, and $D_{\min} = D_c$, $\omega_{\min} = \omega_c$. In figure 1 we display the numerically computed amplitude of B at some fixed time for $D = 9.0$. The $\varepsilon \to 0$ analytic theory, predicts that $\omega = \omega_c$ and $2\theta_F/\pi = 0.58$. Our numerical
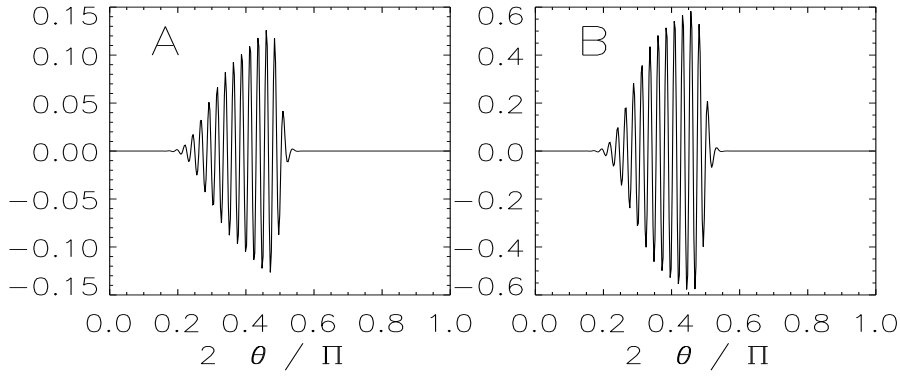
6

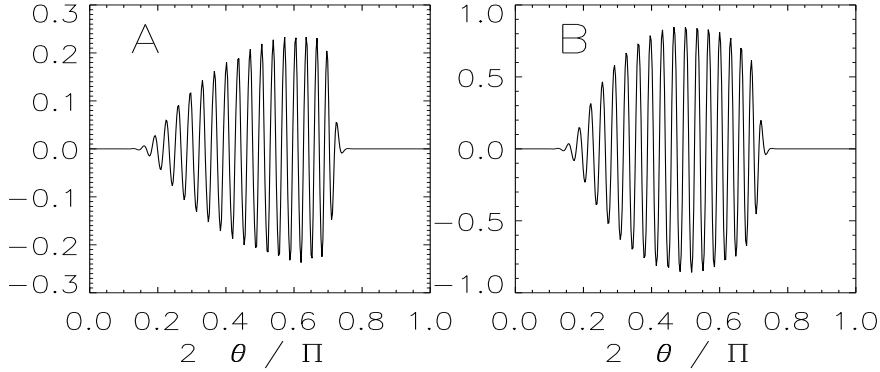*Figure 1.* The case $R_\alpha = 0$, $D = 9.0$.

Figure 2. The case $R_\alpha = 1.0$, $D = 9.0$.

results, which are comparable to those reported by Meunier *et al.* [5], determine $\omega = 1.747$, while the analytic value of θ_F is consistent with figure 1. The front width is seen to be about two wavelengths as illustrated also by Tobias *et al.* [19]. This is a robust feature which is not particularly sensitive to the value of D. On the other hand, the latitudinal range broadens and the amplitude of the magnetic field increases with D.

For the case $R_\alpha = 1$, the asymptotics predicts the values $D_c \approx 7.26$, $\omega_c \approx 1.44$, and $D_{\min} \approx 6.98$, $\omega_{\min} \approx 1.35$. In figure 2, we again plot the numerically integrated B, and it illustrates essentially the same features as figure 1. The realised frequency $\omega = 1.25$ is close to the analytic prediction $\omega = 1.148$, while the front location is visably close to the analytical prediction $2\theta_F/\pi = 0.777$.

The case $R_\alpha = 1.4$ illustrated in figure 3 is particularly interesting because the basic state has bifurcated to the steady α^2-state. The defect
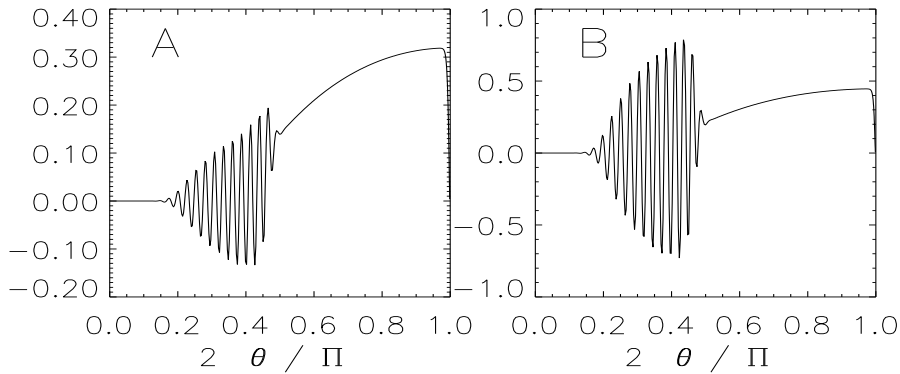
Figure 3. The case $R_\alpha = 1.4$, $D = 9.0$.

visible at the pole is due to the application of zero boundary conditions there. It may be removed by application of more physically realistic boundary conditions but does not affect the results elsewhere. The front is clearly visible riding on the steady state solution. Applying the Dee-Langer condition to formula (9) appropriate to that finite amplitude state determines $\omega = 1.381$, $2\theta_F/\pi = 0.5778$. The numerical results yield $\omega = 1.446$, which together the visibly estimated value of θ_F provide a healthy agreement between the theory and numerics.

Preliminary numerical calculations at higher values of D for various values of R_α suggest that the solution bifurcates and introduces second frequencies; further bifurcations lead on to chaos. An interesting feature is that for given R_α and D, the different frequencies might dominate at different latitudes. Nevertheless, the dominant frequency at the front was always found to be that predicted by our use of the Dee-Langer criterion.

Acknowledgements

References

1. Parker, E.N. (1955) Hydromagnetic dynamo models, *Astrophys. J.*, **122**, pp. 293–314

2. Rüdiger, G. and Arlt, R. (2000) Physics of the solar cycle, in: *Advances in Nonlinear Dynamos*, (Ed. Manuel Núñez and Antonio Ferriz Mas) The Fluid Mechanics of Astrophysics and Geophysics. Vol. 00, pp. 000–000, Gordon and Breach

3. Moss, D., Tuominen, I. and Brandenburg, A. (1990) Buoyancy-limited thin shell dynamos, *Astron. Astrophys.*, **240**, pp. 142–149

4. Kuzanyan, K.M. and Sokoloff, D.D. (1995) A dynamo wave in an inhomogeneous medium, *Geophys. Astrophys. Fluid Dynam.*, **81**, pp. 113–129

5. Meunier, N., Proctor, M.R.E., Sokoloff, D.D., Soward, A.M. and Tobias, S.M. (1997) Asymptotic properties of a nonlinear $\alpha\omega$-dynamo wave: Period, amplitude and latitude dependence, *Geophys. Astrophys. Fluid Dynam.*, **86**, pp. 249–285

6. Griffiths, G.L., Bassom, A.P., Soward, A.M. and Kuzanyan, K.M. (2000) Nonlinear $\alpha^2\Omega$-dynamo waves in stellar shells: I. General structure, *Geophys. Astrophys. Fluid Dynam.*, **93**, pp. 000–000

7. Meunier, N., Nesme-Ribes, E. and Sokoloff, D.D. (1996) Dynamo wave in a $\alpha^2\omega$ dynamo, *Astron. Rep.*, **40**, pp. 415–423

8. Jennings, R.L. (1991) Symmetry breaking in a nonlinear $\alpha\omega-$dynamo, *Geophys. Astrophys. Fluid Dynam.*, **57**, pp. 147–189

9. Tobias, S.M. (1997) Properties of nonlinear dynamo waves, *Geophys. Astrophys. Fluid Dynam.*, **86**, pp. 287–343

10. Worledge, D., Knobloch, E., Tobias, S. and Proctor, M.R.E. (1997) Dynamo waves in semi-infinite and finite domains, *Proc. R. Soc. Lond. A*, **453**, pp. 119–143

11. Soward, A.M. (2000) Thin aspect ratio $\alpha\omega$-dynamos in galactic discs and stellar shells, in: *Advances in Nonlinear Dynamos*, (Ed. Manuel Núñez and Antonio Ferriz Mas) The Fluid Mechanics of Astrophysics and Geophysics. Vol. 00, pp. 000–000, Gordon and Breach

12. Huerre, P. and Monkewitz, P.A. (1990) Local and global instabilities in spatially developing flows, *Annu. Rev. Fluid Mech.*, **22**, pp. 473–537

13. Bassom, A.P., Kuzanyan, K.M. and Soward, A.M. (1999) A nonlinear dynamo wave riding on a spatially varying background, *Proc. R. Soc. Lond. A*, **455**, pp. 1443–1481

14. Le Dizès, S., Huerre, P., Chomaz, J.-M. and Monkewitz, P.A. (1993) Nonlinear stability analysis of slowly-diverging flows: Limitations of the weakly nonlinear approach, in: *Bluff-Body Wakes, Dynamics and Instabilities*, (Ed. H. Eclelmann, J.M.R. Graham, P. Huerre and P.A. Monkewitz) Proceedings of IUTAM Symposium, pp. 147–152, Springer, Berlin

15. Dee, G. and Langer, J.S. (1983) Propagating pattern selection, *Phys. Rev. Lett.*, **50**, pp. 383–386

16. Bassom, A.P. and Soward, A.M. (2000) A nonlinear dynamo wave riding on a spatially varying background: II. Transition from weakly nonlinear to fully nonlinear states, *Proc. R. Soc. Lond. A*, submitted

17. Pier, B., Huerre, P., Chomaz, J-M. and Couairon, A. (1998) Steep nonlinear global modes in spatially developing media, *Phys. Fluids*, **10**, pp. 2433–2435

18. Rüdiger, G. and Arlt, R. (1996) Cycle times and magnetic amplitudes in nonlinear 1D $\alpha^2\Omega$-dynamos, *Astron. Astrophys.*, **316**, pp. L17–L20

19. Tobias, S.M., Proctor, M.R.E. and Knobloch, E. (1997) The rôle of absolute instability in the solar dynamo, *Astron. Astrophys.*, **318**, pp. L55–L58